

# Ultrasonic control of the level of the heterogeneous surface medium in mining

Volodymyr Morkun<sup>1</sup>, Svitlana Hryshchenko<sup>1\*</sup>, Oleksandra Serdiuk<sup>1</sup>, and Andrii Ilnitskyi<sup>1</sup>

<sup>1</sup>Kryvyi Rih National University, 11 Matusyevycha St., 50027 Kryvyi Rih, Ukraine

**Abstract.** Topical One of the major problems of controlling the level of ore or moving fluid (slurry) is recording the reflected signal. Due to evident heterogeneity of the reflecting surface, dispersion of an ultrasonic wave greatly attenuates the reflected signal making it difficult to detect it against random noises. In this case, the only way to solve this problem is application of acoustic reflectors. To analyze this issue, a scheme of the conventional reflector with a radiator-receiver is under study. Efficiency of the acoustic reflector in recording the reflected signal is evaluated. The design of developed recording devices for ultrasonic control over fluid and solid media with heterogeneous surfaces allows increasing their accuracy and reliability due to receiving and transmitting a low-level signal in industrial noises. Industrial testing indicates that the developed ultrasonic device controlling lumpiness of ore materials produces a measuring error of under 1.5%, while efficiency of technological aggregates produced by the ultrasonic method based on measuring the level of the slurry in technological chutes of concentration plants can be evaluated with the  $\pm 1\%$  error.

## 1 Introduction

The level and shape of the surface can be controlled by ultrasonic methods through measuring parameters of volume ultrasonic oscillations and surface Rayleigh and Lamb waves [1 – 8].

In designing means of controlling quantitative characteristics of ore grinding-sorting, application of ultrasound methods based on measuring the period of ultrasonic propagation to the controlled surface is a promising area [9].

In [10], the problem of determining power, pulse-modulated frequency and duration is solved considering the required range of measured distances.

Sounding pulse-modulated power and frequency can be found by means of the generalized characteristic – the coefficient of transferring acoustic oscillations via sound pressure [10]:

$$K_p = \frac{P_n}{P_u}, \quad (1)$$

where  $P_n$  is the amplitude of sound pressure next to the receiving transducer after

---

\* Corresponding author: [aspirodoc@gmail.com](mailto:aspirodoc@gmail.com)

reflecting oscillations from the controlled surface;  $P_u$  is the amplitude of sound pressure in the nearest field of the radiator.

The optimal sounding pulse-modulated frequency is calculated by the expression:

$$f_p = \frac{1.118 \cdot 10^5}{\sqrt{L}}; \quad (2)$$

$$t_i > \frac{1}{\pi \Delta f} \ln \frac{U_y}{U_y - U_n}; \quad (3)$$

$$t_i > \frac{2L_{\min}}{C} - \frac{1}{\pi \Delta f} \ln \frac{U_{\max}}{U_d}, \quad (4)$$

where  $U_y$  is the established value of the amplitude of the sounding pulse;  $\Delta f$  is the pass band of radiated paths and the reception band of the level indicator;  $U_d$  is the discrimination level;  $U_{\max}$  is the maximum amplitude at the output of the reception path;  $L_{\min}$  is the value of the unmeasured area.

As it follows from the above expressions, the level measurement by means of volume ultrasonic oscillations should consider the state of parameters of the environment in which they propagate [9, 12].

To enhance noise-immunity of ultrasound devices of controlling the level of heterogeneous media, some specific waveguides with excited surface Rayleigh waves can be applied [13].

Surface waves are characterized by the greatest interaction with the surrounding environment as their oscillating power is concentrated in the surface layer of the solid body [8, 11, 13]. The buried waveguide with the propagating Rayleigh wave makes part of its energy radiate in the form of extensional ultrasonic oscillations into the liquid that causes abrupt attenuation of the amplitude of oscillations on the surface of the waveguide itself.

The optimal length of the working surface  $l$  assuring the maximum change of the received signal with the waveguide buried into the fluid can be found by the formula:

$$l_{opt} = \frac{C_d}{\alpha_d f} \ln \frac{\frac{\alpha_d + \alpha_l}{C_d} N + (1-N) \frac{\alpha_l}{C_l}}{N \frac{\alpha_l}{C_l} + (1-N) \frac{\alpha_l}{C_l}}, \quad (5)$$

where  $\alpha_l$ ,  $\alpha_t$  and  $\alpha_d$  are coefficients of wave attenuation for extensional, transverse waves and those in the fluid;  $C_l$ ,  $C_t$  and  $C_d$  are velocities of propagation for extensional, transverse waves and those in the fluid;  $f$  is frequency of oscillations;  $N$  is the value depending on the Poisson factor and the material of the rod.

This method can be applied to controlling the media interface under changing pressure and temperature conditions.

Suggests [14] the method of signaling the liquid level of the normal Lamb waves excited in the reservoir wall horizontally in the controlled area. As in the wall of the  $d$  thickness with the constant  $f$  frequency, several propagation modes of normal waves can be excited, the frequency range with  $fd$  not exceeding 3 – 4 MHz·mm is the most admissible.

In this case, only zero modes are excited – the symmetrical  $S_0$  and the asymmetrical  $a_0$ , the attenuation coefficients  $\alpha_{S_0}$  and  $\alpha_{a_0}$  of which are determined by the expressions:

$$\alpha_{s_0} = \frac{\pi^2 f^2 \sigma_1^2 d Z_{1s_0}}{2EC_l}; \quad (6)$$

$$\alpha_{a_0} = \frac{Z_{1a_0}}{4dZ_{a_0}}, \quad (7)$$

where  $Z_{1s_0}$ ,  $Z_{1a_0}$  are normal impedances of the fluid with excited symmetrical and asymmetrical zero modes of waves;  $E$  is the Young module;  $\sigma_1$  is the Poisson factor;  $C_l$  is the velocity of the extensional wave in the plate material.

In practice, the thickness of walls of steel reservoirs is usually 2 – 8 mm. The desired frequency range is within 0.1 – 2 MHz.

Application of ultrasound methods indicates their high efficiency in determining both the level of solid and liquid materials and consumption of fluid harsh media [15 – 18]. The major problem of applying these methods is fixation of the small-amplitude reflected signal under significant noises of various nature.

Evident heterogeneity of the reflecting surface causes great dispersion of an ultrasonic wave that attenuates the reflected signal making it difficult to detect it against some random noises. In this case, the only way to solve this problem is application of acoustic reflectors. To analyze this issue, we study a scheme of the conventional reflector with a radiator-receiver presented in Fig. 1. The given analysis is to determine efficiency of the acoustic reflector in recording a reflected signal. Firstly, it should be noted that analysis of this kind should be conducted after considering characteristics of directivity of radiators and receivers [7, 14].

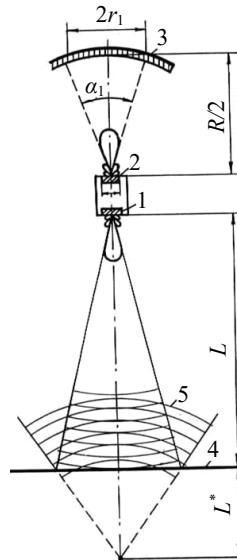


**Fig. 1.** The scheme of the conventional reflector with the receiver-radiator.

Directivity of radiators and receivers is described by the directivity characteristic  $D(\vec{u})$  determined by the ratio of stresses created by an ultrasonic wave at the same distance from the centre of the source or the receiver in the direction of the single radius-vector  $\vec{u}$  and some fixed direction  $\vec{u}_0$ . In practice, the model of this function  $|D(\vec{u})| = \tilde{R}(\vec{u})$  called an

amplitude characteristic of directivity is of particular interest [7, 10]. For a circular-piston radiator directivity is described by the first-order Bessel function, i.e.:

$$\tilde{R}(\alpha) = \left| \frac{2I_1(Z)}{Z} \right|, \quad (8)$$

where  $Z = \frac{\pi d}{\lambda} \sin \alpha$  is a generalized parameter;  $d$  is the piston diameter;  $\alpha$  is the angle off-perpendicular towards the radiator plane;  $\lambda$  is the wave length.

Characteristics of directivity of the same reversible transducer under receiving and radiating modes are the same if amplitude distribution and internal mechanical resistance in terms of electric loads do not change. So, in this case, characteristics of directivity of the receiver and the radiator are described by the same function (1).

Efficiency of the acoustic reflector will be evaluated by means of the  $K_{ef}$  coefficient determined as the ratio of intensity of the ultrasonic wave recorded by the receiver with the reflector available to intensity of the wave recorded without the reflector. In a general case,  $K_{ef}$  will depend on both parameters of the reflector and properties of the dispersing surface. In some approximation, this coefficient can be presented as:

$$K_{ef} = \frac{2\pi \int_0^{r_1} A \tilde{R}^2 \left( \frac{\beta r}{\sqrt{H^2 + (\beta r)^2}} \right) \frac{K_{ref}}{(H^2 + r^2)} \frac{4I_1^2(\alpha r)}{(\alpha r^2)} r dr}{A \tilde{R}^2 \left( d^* / \sqrt{(H^2 - \frac{R}{2})^2 + d^{*2}} \right) K_{ref} \frac{4I_1^2(\alpha d^*)}{(\alpha d^*)^2} \cdot \pi d^2 / 4 (H - \frac{R}{2})^2}, \quad (9)$$

where  $A = \frac{W}{2\pi \tilde{R}(\nu) \sin \nu d \nu}$ ;  $W$  is capacity of the radiator;  $\alpha = \frac{2\pi d}{\lambda R}$ ;  $\beta = \frac{L^*}{L + L^* + \frac{R}{2}}$ ;

$K_{ref}$  is the surface reflection coefficient;  $H = L + L^* + \frac{R}{2}$ .

The parameter  $d^*$  satisfies the condition  $0 < d^* < d$ .

The result (9) is written in some generalized representation with indefinite parameters  $K_{ref}$  and  $L^*$ . As  $K_{ref}$  is determined as a ratio, if:

$$L \gg \frac{R}{2},$$

the efficiency coefficient of the reflector can be evaluated by the formula:

$$\begin{aligned} K_{ef} &\approx \frac{8\pi \int_0^{r_1} \frac{I_1^2(ar) r dr}{(ar)^2}}{(\pi d^2/4)} = 0.219\pi \left( \frac{\lambda R \cdot 3.832}{2\pi d} \right)^2 \bigg/ \left( \frac{\pi d^2}{4} \right) = \\ &= 0.219 \left( \frac{\pi r_1^2}{\pi d^2/4} \right), \end{aligned} \quad (10)$$

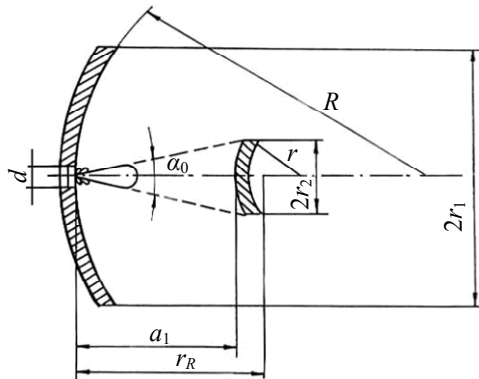
where  $r_1 = \frac{R}{2} \sin \frac{\alpha_0}{2}$ ;  $\alpha_0$  is angle width of the major maximum of directivity of the receiver.

Fig. 1 reveals that  $r_1$  determines the maximum cross size of the spherical mirror. The increased cross size of  $r_1$  will not increase efficiency of the acoustic reflector because of selective directivity of the receiver characteristics. The obtained result (10) is quite evident and indicates that efficiency of the reflector  $K_{ef}$  is proportionate to the ratio of the coverage area of the ultrasonic field by the reflector to the receiver area in the course of recording the sound wave without the reflector. The proportionality coefficient depends on directivity of the receiver. This important result will be used for further evaluation of efficiency of bi-mirror reflectors [16 – 20].

It should be noted that the “conventional scheme” of the acoustic reflector has some disadvantages. Firstly, the receiver-radiator is quite bulky and inconvenient because of different functions of ultrasound receiving and radiating. Secondly, efficiency of the reflector can be improved only due to increasing the radius of the spherical mirror.

## 2 Mathematical representation and description of application

The former disadvantage of this scheme can be corrected due to reversibility of the transducer (Fig. 1) used as a wave receiver-radiator. Yet, it cannot eliminate the latter drawback, so the only solution is to reject the “conventional” scheme in favour of the bi-mirror reflector (Fig. 2).



**Fig. 2.** The bi-mirror reflector.

In this scheme, due to the changed curvature radius of the minor mirror, it is possible to increase the cross size of the large mirror of the reflector that covers the reflected ultrasonic wave without increasing its curvature radius.

It is quite challenging to determine the absolute value of the efficiency coefficient of the bi-mirror reflector, while application of various approximations complicates evaluation of accuracy of the obtained result. So, the only solution of the problem is to determine changes of the efficiency coefficient of the reflector in relation to the acoustic reflector of set geometrical parameters.

At present, acoustic level indicators type of various modifications are being produced. They are intended for noncontact automated remote measurement of the level of bulk and lump materials in nonfood industries for granules of 2 – 200 mm under the temperature of  $-50^{\circ} - +120^{\circ}\text{C}$  [19].

The results of testing level indicators at several industrial enterprises show that their sensitivity and noise-immunity are not sufficient for measuring lump materials. The amplitude of the acoustic signal supplied by a piezoelectric transducer can be greatly increased by focusing the reflected signal by means of the acoustic reflector. The reflector

of the ultrasonic level indicator was chosen as the basic one for further analysis. Its efficiency coefficient is denoted by  $K_{ef}^*$ . In this case, the relative value of  $K_{ef}/K_{ef}^*$  considering (3) can be easily determined through geometrical sizes of the reflectors.

Creation of the bi-mirror reflector places high requirements to geometrical sizes of the system that should be determined in accordance with the laws of geometrical acoustics.

Basic geometrical sizes of the system indicated in Fig. 2 should be determined by:

$$a_1 = \frac{r_R - r + \sqrt{r^2 + r_R^2}}{2}, \quad (11)$$

where  $r_R = R/2$ .

$$r_R = a_1 \operatorname{tg} \frac{\alpha_0}{2}, \quad (12)$$

where  $\frac{\alpha_0}{2} = \arcsin \frac{3.832\lambda}{\pi d}$ ;  $\lambda$  is length of the ultrasound wave.

To determine  $a_1$  and  $r_2$  by the formulae (4) and (5), the radius of the minor mirror  $r$  is set and found from the solution of the equation:

$$\frac{r_1}{r_R \operatorname{tg} \frac{\alpha_0}{2}} = \frac{r_R - r + \sqrt{r^2 + r_R^2}}{r_R + r - \sqrt{r^2 + r_R^2}}, \quad (13)$$

where  $r_1$  is a cross size of the large mirror that can change within:

$$\frac{R}{2} \operatorname{tg} \frac{\alpha_0}{2} < r_1 < R \cdot 0.866. \quad (14)$$

Table 1 presents values of parameters of bi-mirror reflectors of various radii of the large mirror and cross sizes of maximum values (14) as well as the values of the relative efficiency coefficient of reflectors for corresponding geometrical sizes of system parameters.

**Table 1.** Parameters of bi-mirror reflectors.

$r_1$ , mm	$R = 500$ mm				$R = 1000$ mm				$R = 1500$ mm			
	$r_1$ , mm	$a_1$ , mm	$r_1$ , mm	$K_{ef}/K_{ef}^*$	$r_1$ , mm	$a_1$ , mm	$r_1$ , mm	$K_{ef}/K_{ef}^*$	$r_1$ , mm	$a_1$ , mm	$r_1$ , mm	$K_{ef}/K_{ef}^*$
200	158	194	45	1.75	849	319	74	1.59	–	–	–	–
400	74	218	50.7	7.24	317	387	90	6.99	804	523	121	6.68
600	–	–	–	–	201	419	97.3	16.1	475	581	135	15.7
800	–	–	–	–	148	437	101	29.0	343	616	143	28.5
1000	–	–	–	–	–	–	–	–	269	639	148	45.0
1200	–	–	–	–	–	–	–	–	222	655	152	65.2

Parameters  $r$ ,  $a_1$  and  $r_2$  are derivative, i.e. they are determined by the values of  $R$  and  $r_1$  parameters.

For visual demonstration of the influence of geometric sizes of acoustic reflectors on the relative efficiency coefficient  $K_{ef}/K_{ef}^*$ , there is a dependency of this value on the cross size of the large mirror in Fig. 3.

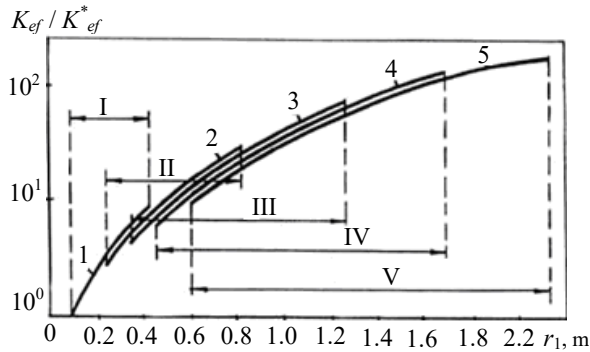


**Fig. 3.** Dependency of the relative efficiency coefficient  $K_{ef}/K_{ef}^*$  on the transverse size of the large mirror.

The arrows indicate areas of possible changes of the  $r_1$  parameter with the corresponding value of the radius of the large mirror  $R$ . As is shown, under  $r_1 = 0.45 \div 0.48$  m, the acoustic reflectors can exceed efficiency of recording reflected signals in relation to the acoustic system of the level indicator.

Thus, by applying the ultrasonic level indicator [19] or its later modifications as the basic one and the acoustic reflector, the sizes of which are chosen according to the data in Table 1, one can greatly improve technical characteristics of the device for measuring the level of materials with the heterogeneous surface.

Let us consider examples of applying ultrasonic control to determining quantitative characteristics of slurry flows. Fig. 4 shows a flow-chart of the automated control system of slurry consumption in the technological chute based on measuring its level in the controlled plane by using the ultrasound method [20 – 22].

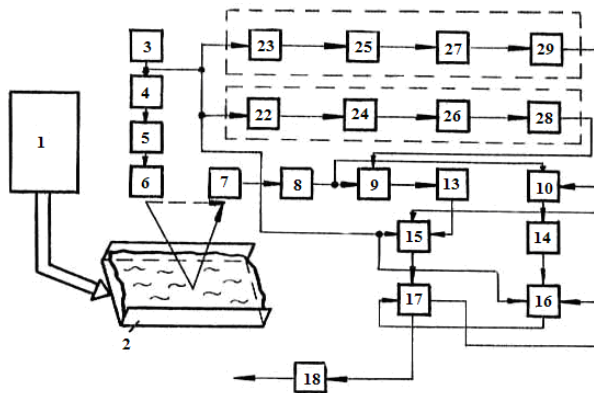


**Fig. 4.** The flow-chart of the automated control system of slurry consumption in the technological chute.

Fig. 4 uses the following notations: 1 is a technological aggregate; 2 is an outlet chute; 3 is a multi-vibrator; 4 is a former; 5 is a generator of sounding impulses; 6, 7 are piezoelectric transducers; 8 is a receiving amplifier; 9, 10 are selection blocks; 11, 12 are time-delay blocks; 13, 14 are starting single vibrators; 15, 16 are timers; 17 is a calculating block; 18 is a scaling block.

The formed ultrasonic signal is transmitted by the piezoelectric transducer 6 towards the slurry flow along the outlet chute 2, is reflected from its surface and comes back to the

receiving piezoelectric transducer 7. The same piezoelectric transducer receives a signal over the air directly from the radiating piezoelectric transducer 6.

The rising edge of the received signal let into by the selection block 9 switches the starting single vibrator 13 that stops the first timer 15. Meanwhile, the first timer 15 measures the time period  $t_1$ :

$$t_1 = S_1 V^{-1}, \quad (15)$$

where  $S_1$  is the distance between the piezoelectric transducers;  $V$  is propagation velocity of ultrasound in the air.

The rising edge of the received signal let into by the selection block 10 switches the starting single vibrator 14, which stops the second timer 16. The second timer 16 measures the time period:

$$t_2 = 2hV^{-1}, \quad (16)$$

where  $h$  is the distance from the piezoelectric transducer 6 to the slurry surface.

In the calculating block 17, there are performed calculations of the slurry level  $H$  in the outlet chute 2:

$$H = S_0 - h = S_0 - \frac{S_1 t_2}{2t_1}, \quad (17)$$

where  $S_0$  is the distance from the piezoelectric transducer 6 to the bottom of the outlet chute 2.

Thus, the calculated value of  $H$  does not depend on fluctuations of the ultrasound propagation velocity.

The level of the slurry flowing in the outlet chute 2 characterized by the constant slope angle and cross-section determines slurry consumption:

$$Q = f(H). \quad (18)$$

Fig. 5 reveals the flow-chart of the automated control system of slurry consumption in the technological chute based on measuring both its level in the controlled plane and its flow speed [18]. This system can be applied to conditions of intensive noises of various nature in the controlled zone.

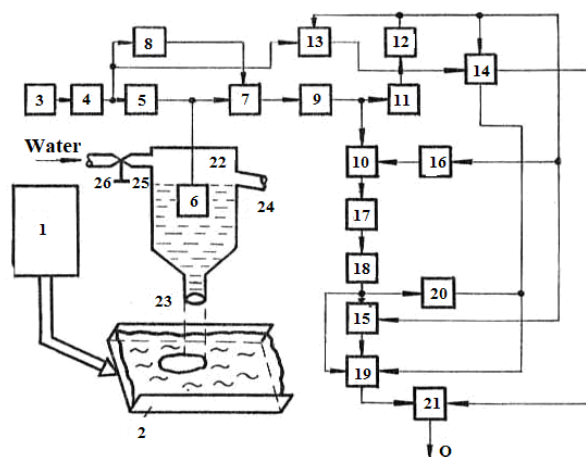


**Fig. 5.** The flow-chart of the automated control system of slurry consumption in the technological chute with both its level and flow speed measured.



Fig. 5 uses the following notations: 1 is a technological aggregate; 2 is an outlet chute; 3 is a multi-vibrator; 4 is a former; 5 is a generator of sounding impulses; 6 is a receiver-radiator piezoelectric transducer; 7, 10 are Schmitt triggers; 12, 16, 18 are single vibrators; 13, 15 are timers; 14, 19 are data storage and selection blocks; 21 is a calculating block; 22 is an accumulating vessel; 23 is a discharge hole; 24 is an overflow tube; 25 is an inlet tube; 26 is a regulating cock to supply and control water flows.

The receiver-radiator piezoelectric transducer 6 is inside the accumulating vessel 22 on its symmetry axis. The accumulating vessel 22 is an empty cylinder constantly filled with water, the bottom of it is a funnel with a discharge hole 23.

The ultrasonic oscillations produced by the receiver-radiator piezoelectric transducer 6 propagate along the water flow draining from the hole 23 towards the outlet chute 2 along which the slurry flows. Where the water flowing from the discharge hole 23 contacts the slurry flowing along the outlet chute 2, there is a zone of the heterogeneous medium in the form of an ellipse stretching towards the slurry moving in the outlet chute 2. If the slurry flow speed is zero, i.e. the slurry rests in the outlet chute 2, the heterogeneous medium zone is a circle the radius of which is almost equal to that of the hole 23 of the accumulating vessel 22.

The ultrasonic oscillations reach the surface of the slurry flow and after being reflected from the external boundary of the heterogeneous ellipse, come back in the same water flow to the receiver-radiator piezoelectric transducer 6.

The time required for ultrasonic oscillations to cover the distance from the receiver-radiator piezoelectric transducer 6 to the external boundary of the heterogeneous zone is proportionate to the level of the slurry  $H$  in the outlet chute 2.

The slurry flowing along the outlet chute 2 carries the heterogeneous medium zone created by the water flowing from the accumulating vessel from the control zone of the receiver-radiator piezoelectric transducer 6. As the length of the heterogeneous ellipse axis is proportionate to the slurry speed, the duration of the received impulse of ultrasonic oscillations is also proportionate to this value.

The second timer 15 records the time  $t_2$  which is proportionate to the speed of the slurry flow in the outlet chute 2. The measurement result is recorded in the second block of data storage and selection 19.

In the calculating block 21 slurry consumption in the technological chute is calculated in a similar way as is shown above.

As is shown the level of the controlled material can be measured by evaluating the value of attenuation of ultrasonic waves propagating along the wall of the technological vessel.

This method can be implemented in three variants:

- measuring parameters of volume ultrasonic oscillations;
- measuring Lamb waves;
- measuring parameters of Rayleigh waves.

In the first case, volume ultrasonic waves are directed so that their multiple reflection inside the metal wall of the vessel occurs. If the controlled material is inside the vessel, there is additional attenuation of the ultrasound which is recorded by the receiver. The methods based on Lamb and Rayleigh waves are more sensitive. In the suggested control method, there are two measuring channels based on Lamb waves, one of which is  $A$  oriented in the horizontal plane in constant contact with the controlled medium (slurry), while the second one ( $B$ ) is oriented in the vertical plane with the same medium the level of which changes under the influence of technological and other factors [8, 21].

Initially, both measuring channels are adjusted so that their output signals be equal if measuring surfaces contact the medium of the same density. As a result, the difference of signals  $\Delta S$  will be equal to zero in this case. With the changes of the level of the controlled medium, the value of the output signal of the  $B$  channel depends on what part of its

measured surface is in contact with the controlled medium. Parameters of this medium do not influence the value  $\Delta S$  due to the correcting impact of the  $A$  channel, this making it possible to apply this method to determining the level of the slurry the density of which varies widely to meet the conditions of the technological process. In a similar way, the measuring method based on Rayleigh waves can be also implemented as in some cases it is applicable to determining lumpy material levels. To initiate Rayleigh waves by the wedge method, the wedge angle is found by the formula [23]:

$$v = \arcsin(C_{wed} \cdot C_R^{-1}), \quad (19)$$

where  $C_{wed}$  is the velocity of extensional waves in the wedge material;  $C_R$  is the velocity of Rayleigh waves in the vessel wall.

The phase velocity of Rayleigh waves is determined from:

$$\eta^6 - 8\eta^4 + 8(3 - 2\xi^2)\eta^2 - 16(1 - \xi^2) = 0, \quad (20)$$

where  $\eta = C_R \cdot C_t^{-1}$ ;  $\xi = C_l \cdot C_t^{-1}$ ;  $C_l$  and  $C_t$  are phase velocities of extensional and transverse waves in the wall of the vessel.

Equation (20) can be converted to:

$$\eta = \sqrt{\frac{16(1 - \xi^2) + 8\eta^4 - \eta^6}{8(3 - 2\xi^2)}}. \quad (21)$$

In this case, it is reduced to  $x = f(x)$  that is solved by the iteration method based on the choice of the initial approximate value  $x_0$  and successive calculation:

$$x_1 = f(x_0), \quad x_2 = f(x_1), \text{ etc.}$$

The series  $x_i$  converges to the required root, if the following condition is fulfilled  $|f'(x)| < 1$ .

The solution of (21) by this method enables finding phase velocity of the Rayleigh waves in the steel sheet and calculating the angle of the wedge made of plexiglass and lead. The calculated angles are  $69^\circ$  and  $47^\circ$  respectively.

Methods of measuring the level of fluid and lumpy materials, quantitative characteristics of slurry- and ore-flows and the design of the devices for their implementation and described in [23 – 28].

### 3 Results and discussion

At the “Kryvbasruda” enterprise, the device controlling the level of ore materials was tested in technological vessels and aggregates. At the concentration plant of Tynnyauzskiy tungsten-molybdenum works, this device was applied to controlling efficiency of technological aggregates by measuring the level of the slurry running in the technological chutes.

The testing covered the device based on the principle of measuring the time period of propagation of ultrasonic oscillations from the transducer to the controlled surface and back and equipped with developed focusing devices and sub-blocks protecting measurement results from technological and operation noises.

The device is characterized by the following operational potentials:

– controlled changes of the noise suppressing zone when measuring time of ultrasonic

oscillation propagation translated for the distance of 0 – 1.5 m;

– controlled changes of the value of the zone of measuring parameters of the received signal in translation to the distance 0 – m (1 – 10 m);

– changes (gradual and phased) of the coefficient of receive path amplification;

– adjustment of the amplitude of the received signal causing the response of the time-delay device; changes in the scale of the analog signal transformation.

The testing error was determined for measuring the level of ore and slurry materials by the ultrasonic control device as well as its convenience and repairability. To assess efficiency of the technological aggregates, the methods given were used.

Industrial testing indicates that the error of the ultrasonic control device used to measure the level of ore materials does not exceed 1.5%.

Accuracy of controlling efficiency of technological aggregates by the ultrasound method based on measuring the slurry level in technological chutes of concentration plants is  $\pm 1\%$ .

## 4 Conclusions

The design of the developed focusing devices for ultrasonic control of the level of fluid and solid media with the heterogeneous surface allows increasing their accuracy and reliability due to receiving and radiating a low-level sounding signal in industrial noises.

The measurement error of the ultrasonic device controlling the level of lumpy ore materials does not exceed 1.5%.

Accuracy of controlling efficiency of technological aggregates by the ultrasound method based on measuring the level of slurry in the technological chutes of concentration plants makes  $\pm 1\%$ .

The authors express their sincere gratitude to Kryvyi Rih National University for support in conducting research.

## References

1. Lynnworth, L.C., & Liu, Y. (2006). Ultrasonic flowmeters: Half-century progress report, 1995-2005. *Ultrasonic*, (44), 1371-1378. <https://doi.org/10.1016/j.ultras.2006.05.046>
2. Baker, R.C. (2016). *Flow Measurement Handbook: Industrial Designs, Operating Principles, Performance, and Applications*. Cambridge University Press. <https://doi.org/10.1017/cbo9781107054141>
3. Medina, C., Segura, J., & De la Torre, Á. (2013). Ultrasound Indoor Positioning System Based on a Low-Power Wireless Sensor Network Providing Sub-Centimeter Accuracy. *Sensors*, 13(3), 3501-3526. <https://doi.org/10.3390/s130303501>
4. Li, D., Ming, F., Huang, X., & Zhang, Y. (2015). Application of Ultrasonic Technology for Measuring Physical and Mechanical Properties of Frozen Silty Clay. *Cold Regions Engineering 2015*. <https://doi.org/10.1061/9780784479315.001>
5. Astashev, V., & Babitsky, V. (2007). *Ultrasonic processes and machines : dynamics, control and applications*. Berlin: Springer.
6. Morkun, V., & Tron, V. (2014). Automation of iron ore raw materials beneficiation with the operational recognition of its varieties in process streams. *Metallurgical and Mining Industry*, (6), 4-7.
7. Morkun, V. Morkun, N. & Pikilnyak, A. (2015) The study of volume ultrasonic waves propagation in the gas-containing iron ore pulp. *Ultrasonics*, (56), 340-343.
8. Morkun, V., Morkun, N., & Pikilnyak, A. (2014) Simulation of the Lamb waves propagation on the plate which contacts with gas containing iron ore pulp in Waveform Revealer toolbox. *Metallurgical and Mining Industry*, (5), 16-19.

9. Morkun, V., Morkun, N., & Pikilnyak, A. (2014). Ultrasonic facilities for the ground materials characteristics control. *Metallurgical and Mining Industry*, (2), 31-35.
10. Krichevskiy, A.G. (1975). Vybory parametrov zondiruyushchikh impul'sov ul'trazvukovykh urovnerov. *Pribory i sistemy upravleniya*, (7), 22-23.
11. Brazhnikov, N.I., Shavykina, N.S., Gordeev, A.P., & Skripalev, V.S. (1975). Ispolzovanie voln Lemba dlya signalizatsii urovnya zhidkikh sred. *Pribory i sistemy upravleniya*, (9), 31-32.
12. Morkun, V., Tron, V., & Goncharov, S. (2015). Automation of the ore varieties recognition process in the technological process streams based on the dynamic effects of high-energy ultrasound. *Metallurgical and Mining Industry*, (2), 31-34.
13. Barsch, M.M., & Morozov V.B. (1975). Poverkhnostnye volny v ul'trazvukovykh indikatorakh urovnya. *Pribory i sistemy upravleniya*, (7), 20-21.
14. Morkun, V., Morkun, N., & Pikilnyak, A. (2014). Ultrasonic phased array parameters determination for the gas bubble size distribution control formation in the iron ore flotation. *Metallurgical and Mining Industry*, (3), 28-31.
15. Morkun, V., Morkun, N., & Pikilnyak, A. (2014). Simulation of high-energy ultrasound propagation in heterogeneous medium using k-space method. *Metallurgical and Mining Industry*, (3), 23-27.
16. Morkun, V., & Tron, V. (2014). Ore preparation energy-efficient automated control multi-criteria formation with considering of ecological and economic factors. *Metallurgical and Mining Industry*, (5), 8-10.
17. Morkun V., & Tcvirkun S. (2014). Investigation of methods of fuzzy clustering for determining ore types. *Metallurgical and Mining Industry*, (5), 11-14.
18. Morkun, V., Morkun, N., Pikilnyak, A. (2014). The gas bubble size distribution control formation in the flotation process. *Metallurgical and Mining Industry*, (4), 42-45.
19. *Pribory dlya izmereniya i regulirovaniya urovnya*. <https://ukrspecavtomat.com.ua/products-category/pribory-dlya-izmereniya-i-regulirovaniya-urovnya/>
20. Morkun, V., Morkun, N., & Pikilnyak, A. (2015). Adaptive control system of ore beneficiation process based on Kaczmarz projection algorithm. *Metallurgical and Mining Industry*, (2), 35-38.
21. Morkun, V., Morkun, N., & Tron, V. (2015). Formalization and frequency analysis of robust control of ore beneficiation technological processes under parametric uncertainty. *Metallurgical and Mining Industry*, (5), 7-11.
22. Golik, V., Komashchenko, V., & Morkun, V. (2015). Geomechanical terms of use of the mill tailings for preparation. *Metallurgical and Mining Industry*, (4), 321-324.
23. Viktorov, I.A. (1966). *Fizicheskie osnovy primeneniya ultrazvukovykh voln Releya i Lemba v tekhnike*. Moskva: Nauka.
24. Golik, V., Komashchenko, V., Morkun, V., & Burdzieva, O. (2015) Metal deposits combined development experience. *Metallurgical and Mining Industry*, (6), 591-594.
25. Golik, V., Komashchenko, V., Morkun, V., & Khasheva, Z. (2015). The effectiveness of combining the stages of ore fields development. *Metallurgical and Mining Industry*, (5), 401-405.
26. Pysmennyi, S., Brovko, D., Shwager, N., Kasatkina, I., Paraniuk, D., & Serdiuk, O. (2018). Development of complex structure ore deposits by means of chamber systems under conditions of the Kryvyi Rih iron ore field. *Eastern-European Journal of Enterprise Technologies*, 5(1-95), 33-45. <https://doi.org/10.15587/1729-4061.2018.142483>.
27. Stupnik, N., Kalinichenko, V., Kolosov, V., Pismenniy, S., & Fedko, M. (2014). Testing complex-structural magnetite quartzite deposits chamber system design theme. *Metallurgical and mining industry*, (2), 89-93.
28. Golik, V., Mitsik, M., Morkun, V., Morkun, N., & Tron, V. (2019). Transportation of concentration and leaching tailings in underground mining of metal deposits. *Mining of Mineral Deposits*, 13(2), 111-120. <https://doi.org/10.33271/mining13.02.111>